# The Missing Link: Synthesis, Crystal Structure, and Thermogravimetric Studies of $InPO_4 \cdot H_2O$

**Xuejiao Tang and Abdessadek Lachgar***

Department of Chemistry, Wake Forest University, Winston-Salem, North Carolina 27109

*Received May 15, 1998*

A new binary indium phosphate monohydrate, $InPO_4 \cdot H_2O$, was synthesized under hydrothermal conditions. Its crystal structure was determined using single-crystal X-ray diffraction methods. $InPO_4 \cdot H_2O$ crystallizes in the triclinic system, space group $P\bar{1}$, with $a = 5.4342(6)$ Å, $b = 5.5508(4)$ Å, $c = 6.5446(5)$ Å, $\alpha = 97.593(6)°$, $\beta = 94.558(6)°$, $\gamma = 107.565(6)°$, and $Z = 2$. The 3-D framework is built from $(In_2O_8(OH_2)_2)$ dimers connected through $(PO_4)$ tetrahedra. Water molecules directly bond to indium. Thermogravimetric studies indicate that $InPO_4 \cdot H_2O$ loses one water molecule in the temperature range between 370 and 480 °C to yield the previously reported anhydrous $InPO_4$. The loss of water corresponds to condensation of the $(In_2O_8(OH_2)_2)$ dimers into linear chains of edge-sharing $(InO_6)$ octahedra. $InPO_4 \cdot H_2O$ represents the missing link between $InPO_4$ and $InPO_4 \cdot 2H_2O$. The structural relationships between $InPO_4 \cdot 2H_2O$, $InPO_4 \cdot H_2O$, $InPO_4$, and other $M^{III}(PO_4) \cdot 2H_2O$ are discussed.

## Introduction

Much interest has been directed toward the search for new open-framework materials due to their potential applications as absorbents, as catalysts in heterogeneous catalysis, as solid-state electrolytes, and as ion exchangers.[1−4] In recent years, research activity in this area has focused on lighter group 13 elements, aluminum and gallium phosphates. Numerous binary aluminophosphates (AlPO) are known for their porous frameworks.[1,5] In addition, many AlPOs and GaPOs with unique chainlike, layered, or three-dimensional open frameworks have been synthesized and structurally characterized.[5−12]

In contrast to the extensive studies of alumino- and gallophosphates, only a few indium phosphates have been reported.[13−19] Most of them are ternary indium phosphates that show interesting structural properties. Their structural types include linear, layered, and three-dimensional open frameworks. To date, only two structurally characterized binary indium phosphates, $InPO_4$ and $InPO_4 \cdot 2H_2O$, have been reported.[20,21] The framework of $InPO_4 \cdot 2H_2O$ is isostructural with $AlPO_4 \cdot 2H_2O$ (variscite).[22] It can be described as a three-dimensional framework built up of $(InO_4(OH_2)_2)$ octahedra linked to each other through $(PO_4)$ tetrahedra. The two water molecules coordinate to indium and are cis with respect to each other. The three-dimensional framework generates six-membered-ring tunnels along the [001] direction and eight-membered-ring tunnels along the [110] direction (Figure 1A). The anhydrous indium phosphate, $InPO_4$, can be directly prepared by slightly changing the synthesis conditions.[20] Its structure is based on infinite linear chains of edge-sharing $(InO_6)$ octahedra. The chains are linked to each other through $(PO_4)$ tetrahedra forming a three-dimensional network (Figure 1B). The sharp structural contrast between the dihydrate, $InPO_4 \cdot 2H_2O$, and the anhydrous $InPO_4$ raises the following questions: Is there an intermediate phase between these two binary indium phosphates? If so, is it a simple indium phosphate monohydrate ($InPO_4 \cdot H_2O$)? Would its structure be less or more open than that of $InPO_4 \cdot 2H_2O$?

Within the framework of our studies of binary and ternary indium phosphates, we attempted to (1) find the right synthesis conditions to stabilize the monohydrate, $InPO_4 \cdot H_2O$; (2) determine its crystal structure and describe the relationships between the three indium phosphate binaries containing 2, 1, and 0 water molecules; and (3) study their thermal behavior using TGA and DTA.

(1) Szostak, R. *Molecular Sieves: Principles of Synthesis and Identification*; Van Nostrand Reinhold: New York, 1989.
(2) Zubieta, J. *Comments Inorg. Chem.* **1994**, *16*, 153−183.
(3) Centi, G.; Trifirò, F.; Ebner, J. R.; Franchetti, V. M. *Chem. Rev.* **1988**, *88*, 55−79.
(4) (a) Clearfield, A. *Chem. Rev.* **1988**, *88*, 125−148. (b) Clearfield, A. *Comments Inorg. Chem.* **1990**, 10, 89−128.
(5) Bennett, J. M.; Marcus, B. K. In *Innovation in Zeolite Materials Science;* Grobet, P. J., et al., Eds.; Elsevier Science Publishers B.V.: Amsterdam, 1987; pp 269−279.
(6) Cowley, A. R.; Chippindale, A. M. *Chem. Commun.* **1996**, 673−674.
(7) Jones, R. H.; Thomas, J. M.; Xu, R.; Huo, Q.; Xu, Y.; Cheetham A. K.; Bieber, D. *J. Chem. Soc., Chem. Commun.* **1990**, 1170−1172.
(8) Chippindale, A. M.; Powell, A. V.; Bull, L. M.; Jones, R. H.; Cheetham, A. K.; Thomas, J. M.; Xu, R. *J. Solid State Chem.* **1992**, *96*, 199−210.
(9) Thomas, J. M.; Jones, R. H.; Xu, R.; Chen, J.; Chippindale, A. M.; Natarajan S.; Cheetham, A. K. *J. Chem. Soc., Chem. Commun.* **1992**, 929−931.
(10) Jones, R. H.; Thomas, J. M.; Huo, Q.; Xu, R.; Hursthouse M. B.; Chen, J. *J. Chem. Soc., Chem. Commun.* **1991**, 1520−1522.
(11) Jones, R. H.; Thomas, J. M.; Chen, J.; Xu, R.; Huo, Q.; Li, S.; Ma Z.; Chippindale, A. M. *J. Solid State Chem.* **1993**, *102*, 204−208.
(12) Esterman, M.; McCusker, L. B.; Baerlocher, C.; Merrouche, A.; Kessler, H. *Nature* **1991**, *352*, 320−323.
(13) Hriljac, J. A.; Grey, C. P.; Cheetham, A. K.; VerNooy, P. D.; Torardi, C. C. *J. Solid State Chem.* **1996**, *123*, 243−248.
(14) Tang X.; Lachgar, A. *Z. Anorg. Allg. Chem.* **1996**, *622*, 513−517.
(15) Chippindale, A. M.;. Brech, S. J. *Chem. Commun.* **1996**, 2781−2782.
(16) Chippindale, A. M.; Brech, S. J.; Cowley, A. R.; Simpson, W. M. *Chem. Mater.* **1996**, *8*, 2259−2264.
(17) Lii, K.-H.; Ye, J. *J. Solid State Chem.* **1997**, *131*, 131−137.
(18) (a) Lii, K.-H. *J. Chem. Soc., Dalton Trans.* **1996**, 815−818. (b) Lii, K. H. *Eur. J. Solid State Chem.* **1996**, *33*, 519−526.
(19) (a) Dhingra, S. S.; Haushalter, R. C. *J. Solid State Chem.* **1994**, *112*, 96−99. (b) Dhingra, S. S.; Haushalter, R. C. *J. Chem. Soc., Chem. Commun.* **1993**, 1665−1667.
(20) Mooney, R. C. L. *Acta Crystallogr.* **1956**, *9*, 113−117.
(21) 1 Mooney-Slater, R. C. L. *Acta Crystallogr.* **1961**, *14*, 1140−1146.
(22) Kniep, R.; Mootz, D.; Vegas, A. *Acta Crystallogr.* **1977**, *B33*, 263−265.

10.1021/ic980548v CCC: $15.00 © 1998 American Chemical Society
Published on Web 11/06/1998

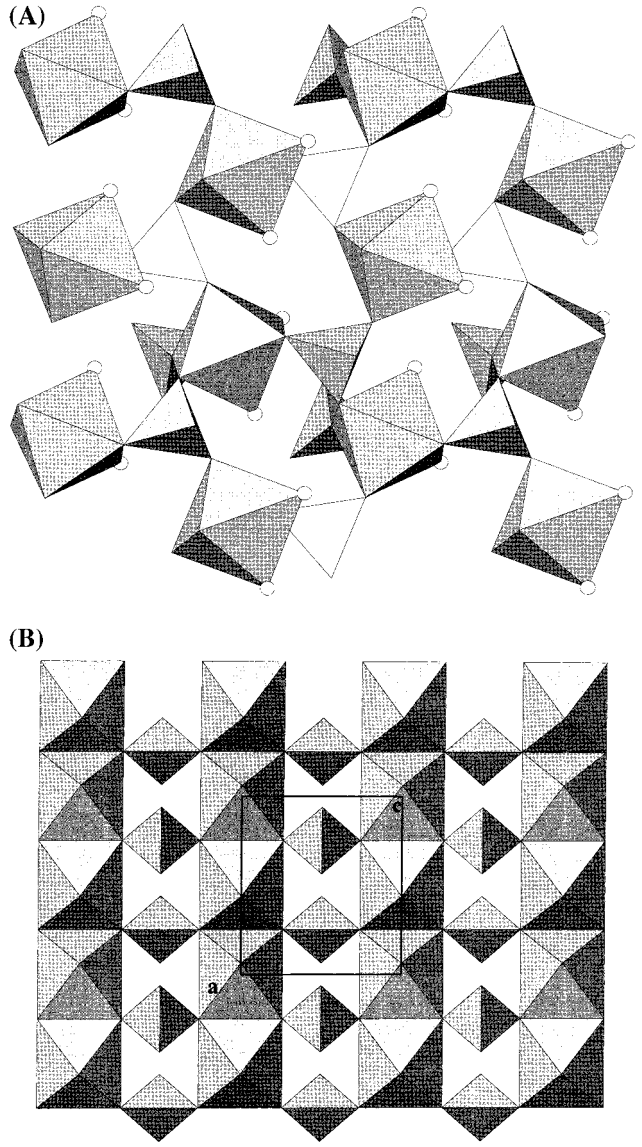


**Figure 1.** (A) View of the structure of $InPO_4 \cdot 2H_2O$ along the [001] direction. (B) View of the structure of $InPO_4$ showing linear chains of edge-sharing ($InO_6$) octahedra connected by ($PO_4$) tetrahedra.

## Experimental Section

**Synthesis.** $KNO_3$ (0.5 mmol) (99+%, Fisher), 0.5 mmol of $InCl_3$ (0.5 M aqueous solution prepared from $InCl_3$, Aldrich, 98%), 3 mmol of $H_3PO_4$ (2 M prepared from concentrated $H_3PO_4$, Fisher, 85% aqueous solution), and $6.25 \times 10^{-2}$ mmol of $CuCO_3 \cdot Cu(OH)_2$ (Fisher, assay (as Cu) 55.7%) were sealed under vacuum in a thick-walled Pyrex tube (length = 112 mm, thickness = 1.5 mm, i.d. = 9 mm, with 40% filling capacity). The reaction was carried out at 200 °C for 60 h, and then the furnace was cooled to room temperature. The product was isolated as colorless needlelike crystals and was later determined to be $InPO_4 \cdot H_2O$. The crystals were vacuum filtered, washed using copious amounts of cold water and acetone, and dried in air at room temperature. The yield of the reaction was found to be 17% based on indium. No solid side products were observed. The use of $KNO_3$ and $CuCO_3 \cdot Cu(OH)_2$ was found to be advantageous in improving the yield of the reaction. $InPO_4 \cdot H_2O$ can also be obtained under similar conditions without the presence of $KNO_3$ and $CuCO_3 \cdot Cu(OH)_2$. The yield, however, is found to be less than 3%.

**Elemental Analysis.** Energy-dispersive X-ray analysis (EDAX) was done using a Philipps 515 scanning electron microscope (SEM). The analysis indicated that the crystals contained In and P in approximately a 1:1 ratio. No K or Cu was found to be present.

**Table 1.** Crystal Data for $InPO_4 \cdot H_2O$

| | |
|---|---|
| formula $InPO_4 \cdot H_2O$ | fw (g/mol) 227.81 |
| $a = 5.4342(6)$ Å | space group $P\bar{1}$ |
| $b = 5.5508(4)$ Å | $T = 298(1)$ K |
| $c = 6.5446(5)$ Å | $\rho_{calcd} = 4.088$ g cm$^{-3}$ |
| $\alpha = 97.593(6)°$, $\beta = 94.558(6)°$, $\gamma = 107.565(6)°$ | $\mu = 67.0$ cm$^{-1}$ (Mo K$\alpha$) |
| $V = 185.07(4)$ Å$^3$ | R1[a] = 0.0308 |
| $Z = 2$ | wR2[b,c] = 0.0628 |

[a] $R1 = \sum||F_o| - |F_c||/\sum|F_o|$ [b] $wR2 = [\sum[w(F_o^2 - F_c^2)^2]/\sum[(wF_o^2)^2]]^{1/2}$. [c] $w^{-1} = \sigma^2(F_o^2) + (0.0091P)^2$ where $P = (\mathrm{Max}(F_o^2,0) + 2F_c^2)/3$.

**Thermal Analysis.** The thermal stability of $InPO_4 \cdot H_2O$ and $InPO_4 \cdot 2H_2O$ was investigated using TGA and DTA. The studies were carried out using a Netzsch STA 409 TGA/DTA apparatus. Samples were heated under a nitrogen flow (22 mL/min) up to 850 °C at 5 °C/min and then cooled to room temperature at 20 °C/min.

**$InPO_4 \cdot H_2O$.** TGA data for $InPO_4 \cdot H_2O$ show a one-step weight loss of 7.7% between 380 and 480 °C. DTA analysis shows the process to be endothermic.

**$InPO_4 \cdot 2H_2O$.** Thermal studies of $InPO_4 \cdot 2H_2O$ were carried out to determine if the compound $InPO_4 \cdot H_2O$ is an intermediate in the dehydration process. Two distinct dehydration steps were found. The first step occurs between 250 and 350 °C and corresponds to a weight loss of 6.4%, and the second step occurs between 380 and 480 °C and corresponds to a weight loss of 6.8%. DTA studies indicate that both dehydration processes are endothermic.

**Infrared Absorption Spectroscopy.** The IR spectrum of $InPO_4 \cdot H_2O$ was recorded using a Perkin-Elmer 1330 infrared spectrophotometer (KBr pellet, cm$^{-1}$): 3200 (s), 1620 (m), 1160 (s), 1020 (s), 915 (s), 785 (m), 625 (m), 570 (s), 485 (m), 370 (w), 325 (m).

**Crystallographic Studies. Single-Crystal X-ray Diffraction Analysis.** The crystal structure of $InPO_4 \cdot H_2O$ was determined using single-crystal X-ray diffraction data collected at room temperature using a Siemens P4 single-crystal diffractometer (Mo K$\alpha$, $\lambda = 0.71073$ Å). A needlelike crystal with approximate dimensions $0.14 \times 0.03 \times 0.03$ mm$^3$ was mounted in a glass capillary for data collection, and 61 reflections ($7° < 2\theta < 41°$) were measured for indexing and cell parameter refinements. The crystal system of $InPO_4 \cdot H_2O$ was determined to be triclinic with the cell parameters $a = 5.4342(6)$ Å, $b = 5.5508(4)$ Å, $c = 6.5446(5)$ Å, $\alpha = 97.593(6)°$, $\beta = 94.558(6)°$, $\gamma = 107.565(6)°$, and $V = 185.07(4)$ Å$^3$. A total of 2672 reflection ($6.4° < 2\theta < 65°$) were collected using the $\theta-2\theta$ scan mode. No intensity decay was observed throughout the data collection. The data were corrected for Lorentz and polarization effects. An empirical absorption correction was applied using $\Psi$-scan data for 11 reflections ($T_{min} = 0.378$, $T_{max} = 0.433$).

The structure was successfully determined in the space group $P\bar{1}$ using direct methods to obtain initial atomic positions. Isotropic least-squares refinements were then carried out (R1 = 0.0355 for 1116 reflections with $F_o > 4\sigma(F_o)$). The final anisotropic full-matrix least-squares refinements were run against $|F|^2$ with 73 parameters to give a structure model with R1 = 0.0308 for 1116 reflections with $F_o > 4\sigma(F_o)$, wR2 = 0.0628, GOF = 1.021. Hydrogen atoms were located from a difference Fourier map. Their coordinates were refined with the constraint $0.77 \leq O-H \leq 0.93$ Å. The maximum and minimum residual electron densities were 1.13 and $-1.15$ e Å$^{-3}$. The Shelxtl version 5 software package was used in the structure determination and refinement. Pertinent crystallographic data are listed in Table 1.

**X-ray Powder Diffraction Studies.** Diffraction studies were carried out using an Enraf-Nonius FR522 Guinier camera and a Phillips X-ray generator with a Cu X-ray tube ($\lambda = 1.54059$ Å). The X-ray powder diffraction pattern of the crystals matched the calculated powder pattern of $InPO_4 \cdot H_2O$; 39 lines ($13° < 2\theta < 56°$) were indexed and used for cell parameter refinement to give the following unit cell parameters: $a = 5.4278(9)$ Å, $b = 5.542(1)$ Å, $c = 6.535(2)$ Å, $\alpha = 97.73(2)°$, $\beta = 94.63(2)°$, $\gamma = 107.57(2)°$, $V = 184.16(5)$ Å$^3$. X-ray powder diffraction of the decomposition product matched that of $InPO_4$.[20]

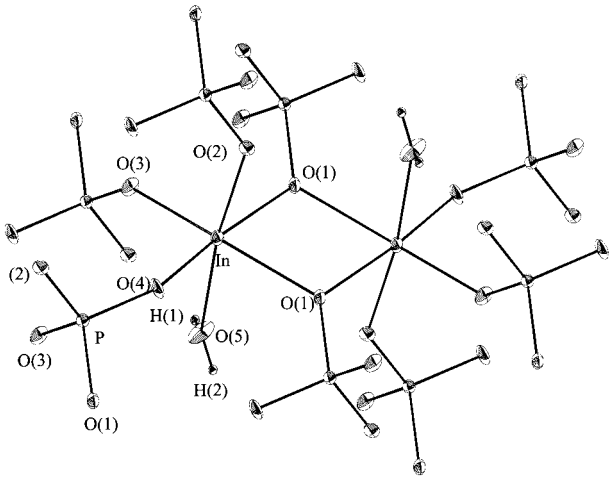


**Figure 2.** Basic building unit of the framework of $InPO_4 \cdot H_2O$ showing a $(In_2O_8(OH_2)_2)$ dimer sharing its eight oxo ligands with eight $(PO_4)$ tetrahedra; 50% thermal ellipsoids.

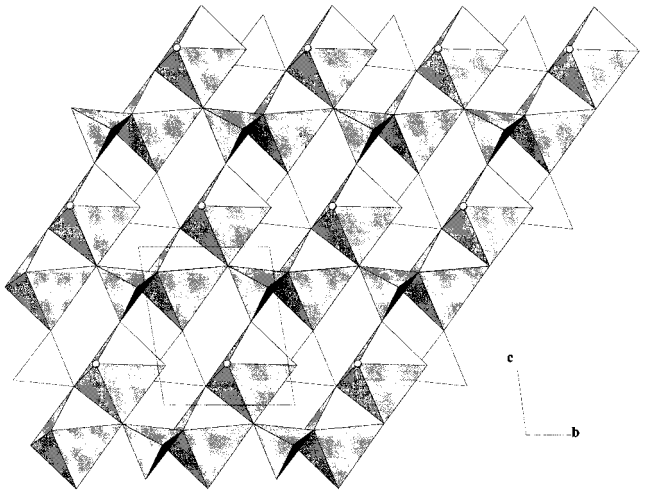


**Figure 3.** View of $InPO_4 \cdot H_2O$ along the [100] direction showing chains of dimers connected to each other through $(PO_4)$ tetrahedra to form layers parallel to the *bc* plane. The small spheres represent water molecules (O(5)) coordinating to indium.

## Results and Discussion

**Crystal Structure Description.** The compound $InPO_4 \cdot H_2O$ has a neutral three-dimensional framework built up from $(In_2O_8(OH_2)_2)$ dimers linked to each other through $(PO_4)$ tetrahedra. Each indium atom coordinates to five oxo ligands and one aquo ligand to form a distorted $(InO_5(OH_2))$ octahedron. The shortest and longest In−O bond distances are In−O(4) = 2.069(4) Å and In−O(1) = 2.230(3) Å. Each $(InO_5(OH_2))$ octahedron at $(x, y, z)$ is linked to its equivalent octahedron at $(1 - x, 1 - y, -z)$ through two oxygen O(1) ligands $(x, y, z; 1 - x, 1 - y, -z)$ to form edge-sharing $(In_2O_8(OH_2)_2)$ dimers (Figure 2). The shared edge constitutes the shortest oxygen−oxygen distance within the dimer (O(1)−O(1) = 2.716(7) Å), whereas the longest edge within the dimer is found to be O(2)−O(3) = 3.299(6) Å. The distance between the two In atoms of the dimer is 3.500(1) Å, similar to that found in $(In_2O_{10})$ dimers in $CaIn_2(PO_4)_2(HPO_4)$ (3.483(6) Å).[14] Each $(In_2O_8(OH_2)_2)$ dimer shares eight oxo ligands (two O(1), two O(2), two O(3), and two O(4)) with eight $(PO_4)$ tetrahedra. Two water molecules (O(5)) constitute the two unshared corners of the dimer (Figure 2). The dimers are aligned along the [011] direction and form layers parallel to the *bc* plane (Figure 3). The $(PO_4)$ tetrahedra connect three neighboring dimers within the same plane through their O(1), O(2), and O(4) oxo ligands, and adjacent dimer layers are linked to each other through the remaining oxo ligand (O(3)). The shortest and longest P−O distances are P−O(4) = 1.513(4) Å and P−O(1) = 1.574(4) Å. The three-dimensional framework thus formed generates six-membered-ring opening tunnels (three $(InO_5(OH_2))$ and three $PO_4$) running along the [001] direction. Investigation of the environment around O(5), H(1), and H(2) indicates that hydrogen bonds are formed within the tunnels (Figure 4). Atomic coordinates and selected bond distances and angles are listed in Tables 2 and 3.

Bond valence sum calculations[25] confirm the +3 and +5 oxidation states for In and P, respectively ($\sum s = 3.13$ for In, and $\sum s = 4.96$ for P). The ligands O(1), O(2), O(3), and O(4) bond to indium and phosphorus atoms, and their bond valence summations range from 1.79 to 2.00 (O(1), 2.00; O(2), 1.79; O(3), 1.82; O(4), 1.98). In contrast, the bond valence sum for O(5) is found to be 0.51 when hydrogen atoms are not taken into consideration.

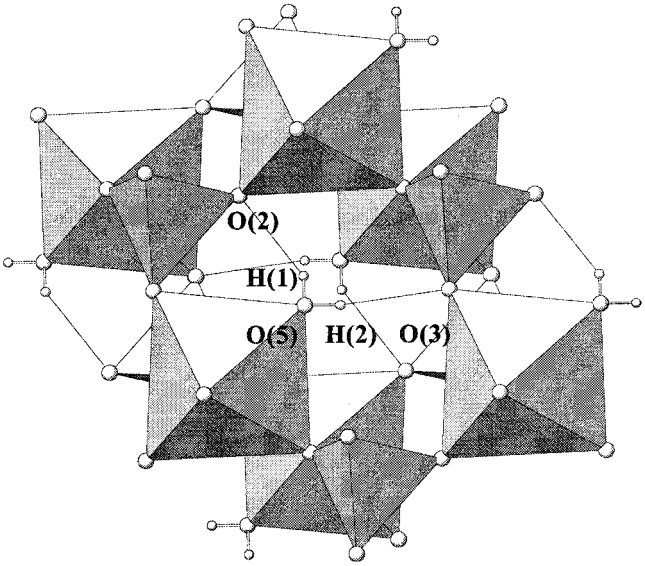


**Figure 4.** View of a portion of the framework of $InPO_4 \cdot H_2O$ showing hydrogen bonding within the tunnels.

**Table 2.** Fractional Atomic Coordinates, $U$(eq),[a] for $InPO_4 \cdot H_2O$

| | *x* | *y* | *z* | *U*(eq) (Å$^2$) |
|---|---|---|---|---|
| In | 0.14013(7) | 0.73305(7) | 0.21978(6) | 0.0067(1) |
| P | 0.7694(2) | 1.1243(2) | 0.2559(2) | 0.0058(2) |
| O(1) | 0.1405(7) | 0.6600(6) | −0.1188(5) | 0.0082(6) |
| O(2) | −0.1670(7) | 0.8863(7) | 0.1585(5) | 0.0082(6) |
| O(3) | 0.4731(7) | 1.0626(7) | 0.2520(6) | 0.0097(6) |
| O(4) | 0.0817(7) | 0.7688(7) | 0.5295(5) | 0.0109(7) |
| O(5) | 0.4155(8) | 0.5336(8) | 0.2613(8) | 0.0189(9) |
| H(1)[b] | 0.53(1) | 0.57(1) | 0.20(1) | 0.02(1) |
| H(2)[b] | 0.42(1) | 0.41(1) | 0.28(1) | 0.01(1) |

[a] $U$(eq) is defined as one-third of the trace of the orthogonalized $\mathbf{U}_{ij}$ tensor. [b] Hydrogen atoms are refined with the restriction 0.77 Å ≤ O−H ≤ 0.93 Å.

**Infrared Studies.** The IR spectroscopic studies of $InPO_4 \cdot H_2O$ reveal a strong and relatively broad absorption band at 3200 cm$^{-1}$ characteristic of an O−H stretch vibration. The absorption band at 1620 cm$^{-1}$ had been observed in $MPO_4 \cdot$

(23) Tarte D.; Paques-Ledent, M. Th. *Bull. Soc. Chim. Fr.* **1968**, 1750−1756.
(24) Deichman, E. N.; Ezhova, Zh. A.; Tananaev, I. V.; Kharitonov, Yu. Ya. *Russ. J. Inorg. Chem.* **1974**, 19−21.
(25) Altermatt, D.; Brown, I. D. *Acta Crystallogr.* **1985**, *B41*, 240−244.

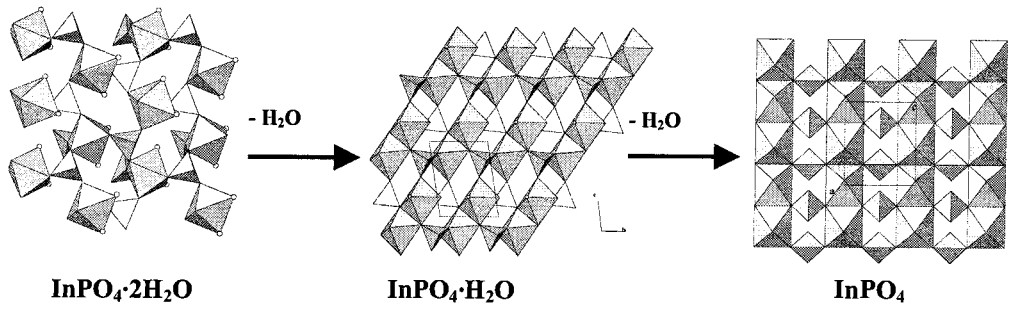


**Figure 5.** Structural transformation taking place during the dehydration process of $InPO_4 \cdot 2H_2O$ to form the anhydrous $InPO_4$.

**Table 3.** Selected Bond Distances (Å) and Angles (deg) for $InPO_4 \cdot H_2O$[a]

| $InO_6$ Octahedron | | | | | | |
|---|---|---|---|---|---|---|
| In | O(4) | O(3) | O(2) | O(5) | O(1) | O(1)[a] |
| O(4) | 2.069(4) | 96.5(2) | 88.6(2) | 93.7(2) | 171.4(2) | 97.2(2) |
| O(3) | | 2.122(3) | 102.0(2) | 84.7(2) | 91.5(2) | 162.6(2) |
| O(2) | | | 2.124(3) | 172.7(2) | 86.7(2) | 89.2(2) |
| O(5) | | | | 2.134(3) | 90.2(2) | 83.7(2) |
| O(1) | | | | | 2.200(3) | 75.6(2) |
| O(1)[a] | | | | | | 2.230(3) |

| $PO_4$ Tetrahedron | | | | |
|---|---|---|---|---|
| P | O(4)[b] | O(2)[c] | O(3) | O(1)[d] |
| O(4)[b] | 1.513(4) | 111.2(2) | 113.3(2) | 106.7(2) |
| O(2)[c] | | 1.536(3) | 110.0(2) | 108.8(2) |
| O(3) | | | 1.539(4) | 106.7(2) |
| O(1)[d] | | | | 1.574(4) |

| H Bonds | | | |
|---|---|---|---|
| O(5)−H(1) | 0.74(8) | O(3)[e]−H(2) | 2.05(8) |
| O(5)−H(2) | 0.69(8) | O(5)−O(2)[c] | 2.710(4) |
| O(2)[c]−H(1) | 2.08(8) | O(5)−O(3)[e] | 2.719(4) |
| ∠O(5)H(1)O(2)[c] | 143(7) | ∠O(5)H(2)O(3)[e] | 163(7) |

[a] Symmetry code: (a) $-x, -y + 1, -z$; (b) $-x + 1, -y + 2, -z + 1$; (c) $x + 1, y, z$; (d) $-x + 1, -y + 2, -z$; (e) $x, y - 1, z$.

$2H_2O$, $MAsO_4 \cdot 2H_2O$ (M = Fe, Al, In, Tl), and $InAsO_4 \cdot 4H_2O$[23,24] and is assigned to the libration vibration of water. The presence of these two absorption bands confirms that the title compound contains water of crystallization. The absorption bands between 1200 and 900 $cm^{-1}$ and 650−480 $cm^{-1}$ are attributed to the P−O bond stretch and deformations.

**Thermal Stability Studies.** The dehydration of $InPO_4 \cdot H_2O$ is found to occur at a relatively high temperature, ~380 °C, to give $InPO_4$ (weight loss of 7.7%). In contrast, $InPO_4 \cdot 2H_2O$ is found to dehydrate in two steps. The first step occurs between 250 and 350 °C and corresponds to a weight loss of 6.4%, consistent with a loss of one water molecule to give the monohydrate $InPO_4 \cdot H_2O$. Subsequently the compound loses a second water molecule between 380 and 480 °C to give the anhydrous $InPO_4$, which is found to be stable up to 1000 °C (the maximum temperature reached during TGA studies). Both dehydration processes are found to be endothermic. The products of the thermal decomposition were characterized by X-ray powder diffraction.

step 1:

$$InPO_4 \cdot 2H_2O \rightarrow InPO_4 \cdot H_2O + H_2O$$

~250 °C: % loss calcd, 7.3; exptl, 6.4

step 2:

$$InPO_4 \cdot H_2O \rightarrow InPO_4 + H_2O$$

~380 °C: % loss calcd, 7.9; exptl, 7.7

The structures of $InPO_4 \cdot 2H_2O$, $InPO_4 \cdot H_2O$, and $InPO_4$ are closely related (Figure 5). The structural transformation occurring during the dehydration process of $InPO_4 \cdot 2H_2O$ can be interpreted as successive condensations of octahedra resulting from loss of aquo ligands followed by rearrangement of the environment around indium to satisfy its octahedral coordination requirements. In the first step of the dehydration process, the $(InO_4(OH_2)_2)$ octahedra in the $InPO_4 \cdot 2H_2O$ framework lose one aquo ligand and condense through edge-sharing to form the dimers $(In_2O_8(OH_2)_2)$ found in the framework of $InPO_4 \cdot H_2O$. Subsequently, these dimeric units lose their aquo ligands and condense to form linear chains of edge-sharing octahedra found in the structure of the anhydrous $InPO_4$.

## Conclusion

The structure of $InPO_4 \cdot H_2O$ is novel and has no equivalent among alumino- or gallophosphates. This is rather unusual, since phosphates of group 13 elements tend to form isotypic series. For example, the crystal structures of $TlPO_4 \cdot 2H_2O$ and $TlPO_4$ are the same as their indium phosphate equivalents.[20,21] The structure of $AlPO_4 \cdot 2H_2O$ is isotypic with that of $InPO_4 \cdot 2H_2O$.[22] The structural chemistry of In(III) phosphates has a closer relationship to that of transition metal phosphates. Anhydrous transition metal phosphates with the general formula $MPO_4$ (M = $Ti^{3+}$, $V^{3+}$, $Cr^{3+}$) are isostructural with $InPO_4$.[26,27] The dihydrate transition metal phosphates, such as $VPO_4 \cdot 2H_2O$ and $FePO_4 \cdot 2H_2O$, have the same structural properties as $InPO_4 \cdot 2H_2O$.[28−31] However, $InPO_4 \cdot H_2O$ is the only known binary metal phosphate that contains $(M_2O_8(OH_2))$ dimers. In contrast, the framework of $VPO_4 \cdot H_2O$ is built by chains of corner-sharing $VO_6$ octahedra (oxygen atom of the water molecule connects vanadium octahedra into V−O−V chains) and $PO_4$ tetrahedra.[32] The vanadium phosphate $(VO)_2(P_2O_7) \cdot 2H_2O$ contains dimers of face-sharing octahedra, while the anhydrous $(VO)_2(P_2O_7)$ contains $(M_2O_{10})$ dimers linked to each other via corner sharing to form double chains.[36,37] The

(26) Glaum, R.; Reehuisy, M.; Stüsser, N.; Kaiser, U.; Reinauer, F. *J. Solid State Chem*. **1996**, *126* (1), 15−21.
(27) Attfield, J. P.; Battle, P. D.; Cheetham, A. K. *J. Solid State Chem*. **1985**, *57*, 357−361.
(28) Schindler, M.; Joswig, W.; Baur, W. H. *Eur. J. Solid State Inorg. Chem*. **1995**, *32*, 109−120.
(29) Moore, P. B. *Am. Mineral*. **1966**, *51*, 168−176.
(30) Kitahama, K.; Kiriyama, R.; Baba, Y. *Acta Crystallogr*. **1975**, *B31*, 322−324.
(31) X. Tang and A. Lachgar, to be published.
(32) Vaughey, J. T.; Harrison, W. T. A.; Jacobson, A. J.; Goshorn, D. P.; Johnson, J. W. *Inorg. Chem.* **1994**, *33*, 2481−2487.
(33) Aranda, M. A. G.; Bruque, S.; Attfield, J. P. *Inorg. Chem.* **1991**, 2043−2047.
(34) Botelho, N. F.; Roger, G.; d'Yvoire, F.; Moêlo, Y.; Volfinger, M. *Eur. J. Mineral*. **1994**, *6*, 245−254.
(35) Kniep, R.; Mootz, D. *Acta Crystallogr*. **1973**, *B29*, 2292−2294.
(36) Gorbunova, Yu. E.; Linde, S. A. *Sov. Phys.-Dokl. (Engl. Transl.)* **1979**, *24*, 138.

**Table 4.** Structure Types of Binary M(III) Phosphates and Arsenates

| structure type | space group | compounds | refs |
|---|---|---|---|
| $InPO_4$ | *Cmcm* | $InPO_4$, $TlPO_4$, $TiPO_4$, $VPO_4$, $\beta$-$CrPO_4$ | 20, 26, 27 |
| $InPO_4 \cdot H_2O$ | $P\bar{1}$ | $InPO_4 \cdot H_2O$ | this work |
| $VPO_4 \cdot H_2O$ | *C*2/*c* | $VPO_4 \cdot H_2O$, $MnPO_4 \cdot H_2O$, $MnAsO_4 \cdot H_2O$ | 32, 33 |
| variscite | *Pbca* | $InPO_4 \cdot 2H_2O$, $AlPO_4 \cdot 2H_2O$, $TlPO_4 \cdot 2H_2O$, $InAsO_4 \cdot 2H_2O$, $FeAsO_4 \cdot 2H_2O$, $TlAsO_4 \cdot 2H_2O$ | 21, 22, 34, 30 |
| metavariscite | $P2_1/n$ | $InPO_4 \cdot 2H_2O$, $AlPO_4 \cdot 2H_2O$, $VPO_4 \cdot 2H_2O$, $FePO_4 \cdot 2H_2O$ | 28, 29, 31, 35 |

formation of ($In_2O_{10}$) dimers has been observed in ternary indium phosphates $CaIn_2(PO_4)_2(HPO_4)$[14] and $SrIn_2(PO_4)_2(HPO_4)$.[38] Table 4 summarizes the crystallographic data of known binary M(III) phosphates and arsenates.

Water molecules coordinated to In atoms are found in $InPO_4 \cdot 2H_2O$,[21] $Cs[In_2(PO_4)(HPO_4)_2(H_2O)]$,[19] and $[In_8(HPO_4)_{14}(H_2O)_6](H_2O)_5(H_3O)(C_3N_2H_5)_3$.[16] In these three compounds, aquo ligands constitute the unshared corners of ($InO_6$) octahedra. In each compound, the longest In−O bond is that between In and the water molecule (2.20−2.28 Å).

Hydrothermal synthesis can be advantageously used to stabilize intermediates in mono- or microcrystalline forms in order to study their crystal structures using single-crystal or powder X-ray diffraction techniques. In our laboratory, systematic synthetic investigations of ternary indium and mixed indium−iron phosphates using hydrothermal synthesis methods led to the characterization of a number of new phases with novel structural properties. Studies of their thermal stability, ion exchange properties, and ionic conductivity are underway.

**Acknowledgment.** We thank Mr. Heinz-Jürgen Kolb from the Department of Chemistry, University of Tübingen, FRG, for TGA and DTA data collection. The financial support of Wake Forest University through the Research and Creativity grant is greatly appreciated.

**Supporting Information Available:** Tables listing crystal data, atomic coordinates, isotropic and anisotropic displacement parameters, and bond lengths and angles (4 pages). Ordering information is given on any current masthead page.

IC980548V

(37) (a) Torardi, C. C.; Calabrese J. C. *Inorg. Chem.* **1984**, *23*, 1310−1320. (b) Nguyen, P. T.; Hoffman, R. D.; Sleight, A. W. *Mater. Res. Bull.* **1995**, *9*, 1055−1063.

(38) X. Tang and A. Lachgar, to be published.